Comparison and Analysis of Toroidal and Classic Propellers

Luka Žagar[1], Marko Jamšek[2]

[1] *Gimnazija Vič, 1000 Ljubljana, Slovenia*
[2] *Laboratory for Neuromechanics and Biorobotics, Department of Automation, Biocybernetics and Robotics*
Jožef Stefan Institute, Ljubljana, Slovenia
E-mail: lukazagar64@gmail.com

Abstract: *This paper compares and analyses the performance characteristics of toroidal and classic propellers for air-driven propulsion applications. The study includes the theoretical background on these propellers' design principles and fluid dynamics behaviour. Experimental investigations were conducted in a specially designed test setup for air-driven propellers. The results highlight the efficiency, thrust generation, noise generation and power consumption differences between the two propeller types. Our results indicate that toroidal propellers have the potential to achieve higher thrust efficiency and performance for a given diameter. These findings offer valuable insights for choosing a suitable propeller design for various air-driven propulsion applications.*

1 Introduction

Propellers are crucial components in both aviation and marine propulsion systems, driving aircraft and vessels through their respective mediums. The traditional design of classic propellers has been prevalent for many years, while toroidal propellers represent a more innovative and promising approach [1]. Classic propellers, otherwise commonly known as axial-flow propellers, are widely used in both aviation and marine applications. Their design is based on the principles of helical lifting surfaces, where the blades generate thrust by inducing a pressure difference between the forward and rearward sides [2]. Classic propellers operate on the same fundamentals in air and water, with variations in design to accommodate the differences in fluid properties.

Toroidal propellers represent an innovative design that has gained attention in recent years. The unique toroidal shape of the blades allows for improved fluid dynamics and reduced losses due to vortex formation and tip cavitation [3], [4]. Toroidal propellers offer distinct advantages in both air and water, promising enhanced hydrodynamic efficiency and performance.

The toroidal design of the propeller blades often leads to a higher weight compared to traditional axial-flow propellers. This weight disparity is primarily attributed to the complex geometry and increased material volume required to construct the closed-loop blade structure. As a result, the increased weight of toroidal propellers may pose challenges in applications where weight constraints are critical.

The unique shape of toroidal propellers presents manufacturing complexities that go beyond traditional propeller production methods. Fabricating blades with toroidal geometry requires advanced manufacturing techniques, such as 5-axis CNC machining or additive manufacturing (sintering technology). These specialized processes add complexity to the manufacturing process and can increase production costs, which may limit the widespread adoption of toroidal propellers [1].

The selection of materials for toroidal propellers is critical to achieving the desired balance between weight, strength, and durability. The complex geometry of the blades may require advanced materials or composites to ensure adequate structural integrity under operational loads. Balancing these material considerations is essential to optimizing the performance and longevity of toroidal propellers.

This research aims to compare and analyse the performance of toroidal and classic propellers in air-driven applications.

2 Experimental Setup

The study consisted of the evaluation of four distinct propeller designs. The propeller name “NACA2415” refers to an airfoil design profile developed by the National Advisory Committee for Aeronautics (NACA). The designation "NACA2415" provides information about the airfoil's shape. The first two digits, "24" indicate that the airfoil has a thickness-to-chord ratio of 24%, while the last two digits, "15" indicate that the maximum camber (curvature of the upper surface) occurs at 15% of the chord length from the leading edge.

The propellers, presented in **Figure 1**, were:
- 6040 NACA2415 Classic Propeller [A],
- 6040 NACA2415 TriLoop Toroidal Propeller [B],
- 6040 NACA2415 Toroidal Propeller [C],
- 7x4 SF APS Propeller [D].

Figure 1: A: 6040 NACA2415 Classic Propeller, B: 6040 NACA2415 TriLoop Toroidal Propeller, C: 6040 NACA2415 Toroidal Propeller, D: 7x4 SF APS Propeller

2.1 Propeller design and manufacture

The experiment involved the fabrication of toroidal propellers utilizing advanced manufacturing techniques. The propellers were modelled based on the NACA2415 airfoil [5], [6]. The propeller size and pitch were scaled to 6040 dimensions and were designed using Fusion 360 software.

The fabrication process was carried out using Stereolithography (SLA) technology. A layer resolution of 0.010 mm was used during the printing process, ensuring intricate detailing of the toroidal blade geometry. As a printing material, 3DJAKE Basic Resin was selected for having favourable mechanical properties for the experimental objectives. The cured material has a density of 1.18 g/cm³, a tensile strength of 3730 MPa, and an impact strength of 12 KJ/m² [7].

2.2 Test Stand Specifications

The measurements were conducted using a custom-designed test stand shown in **Figure 2**.

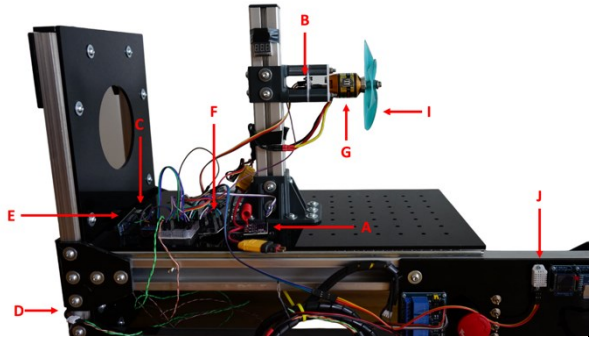

Figure 2: A: INA3221 sensor board, B: AS5600 sensor, C: Load-cell, D: HX711 board, E: Arduino Nano, F: ESP32, G: AXI 2820/14 motor, I: Tested propeller, J: DHT22

The test stand incorporated instrumentation to obtain real-time data for bus and load voltage, current draw [INA3321sensor board], motor speed [AS5600 sensor], applied load [Loadcell & HX711 board] and other ambient parameters [DHT22].

To accurately measure the thrust produced by the motor, we used a 20 kg load cell of the Parallel Beam Strain Gauge type with a rated precision of ± 0.05% Full Scale and a rated output of 1.0 ± 0.15 mV/V.

The load cell's signal was measured using an HX711 board equipped with a 24-bit A/D converter, running at 80 Hz. The HX711 board features an on-chip active low-noise Programmable Gain Amplifier with selectable gain, ensuring precise and reliable measurements.

For current measurements, we utilized the INA3221 board, with a custom shunt resistor to support currents up to 30 A. The INA3221 board exhibits a gain error of 0.25% (maximum) and provides high-resolution current measurement at 10 mA resolution. Additionally, it offers 8 mV resolution for bus and load voltage measurements, contributing to accurate power evaluations.

To monitor the ambient parameters such as humidity and temperature during the experiments, we employed the DHT22 sensor. The DHT22 sensor has a relative humidity measurement range of 0-100% with an accuracy of 5% and a relative temperature measurement within a range of -40 to 80 °C, with an accuracy of ± 0.5 °C.

To obtain RPM readings, we utilized the AS5600 magnetic rotary position sensor. This sensor boasts a resolution of 12 bits, equating to an angle resolution of 0.35 degrees, enabling RPM data collection.

For motor power values and overall data processing, we used the ESP32, a versatile microcontroller with a 16-bit Pulse-Width Modulation (PWM) resolution. The ESP32 also performed data processing tasks for all the sensors.

The motor used in the experiments was an AXI 2820/14 GOLD LINE. This motor features an RPM/V rating of 860, with a maximum efficiency of 86% and an internal resistance of 78 mΩ. The motor was selected based on its compatibility with much larger and more aggressive propellers, ensuring that the motor itself did not significantly impact the experiment's outcomes and results.

The measurements were captured at a frequency of 60 Hz due to the HX711 limitations. This sampling rate allowed sufficient tracking of dynamic changes and really basic transient effects throughout the motor's operational spectrum.

2.3 Experimental protocol

The experimental protocol consisted of running the motor from nominal speeds to an upper threshold of 11 000 RPM within a duration of 150 s. The motor underwent controlled incremental ramp-ups every 1500 ms, with PWM signal increments of 10 µs (standard protocol), corresponding to approximately 1% of power per step within the PWM range of 1000 µs to 2000 µs (maximum power output (dead zone) was hit at around 1810 µs based on the ESC threshold calibration and ESC PWM range reading and scaling).

Upon reaching the maximum RPM, the motor sustained this level for approximately 30 s. During this steady-state part, we evaluated the maximum thrust produced by each propeller. The experimental procedure was repeated 3 times for each propeller type.

3 Results

3.1 Thrust measurements

One example of the thrust measurement during the experiment for each propeller type is shown in **Figure 3**. The maximum value of trust for each propeller type was calculated by averaging the data from the last 20 s of the measurement as indicated by the shaded zone. A violin plot of all the measured values used for these calculations is presented in **Figure 4**. Overall, we observed that the 6040 NACA2415 Classic Propeller exhibited the lowest thrust levels at the maximum speed of the motor at 2.1 ± 0.1 N (mean ± SD). The 6040 NACA2415 Toroidal Propeller achieved a slightly improved thrust of

2.2 ± 0.1 N, while the 6040 NACA2415 TriLoop Toroidal Propeller further enhanced thrust generation, reaching 2.7 ± 0.1 N. Notably, the 7x4 SF APS Propeller displayed the highest maximum thrust among the tested propellers of 3.6 ± 0.2 N.

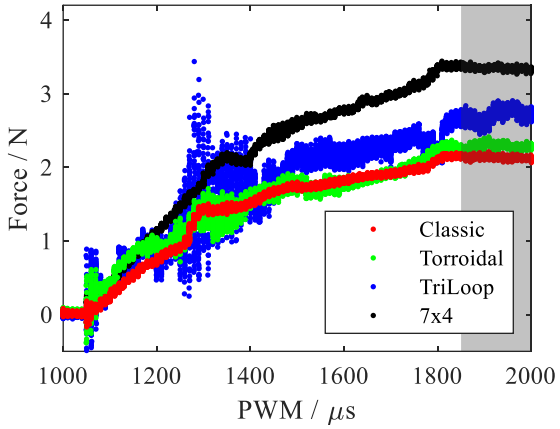

Figure 3: Example of thrust measurements for each propeller type over the course of the experiment. The highlighted section indicates data that was used to calculate the maximum produced thrust.

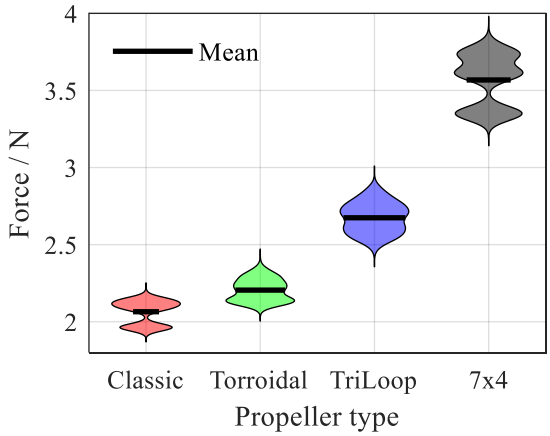

Figure 4: Violin plot of the maximum thrust for each propeller type (three measurements per propeller).

These results show, that the 6040 NACA2415 TriLoop Toroidal Propeller demonstrated better maximum thrust per specific diameter compared to the classic propeller configurations. This suggests that toroidal propellers have the potential to achieve higher thrust efficiency and performance within a given propeller diameter. However, the 7x4 SF APS Propeller's exceptional performance must not be overlooked. The increased size of the propeller contributes to greater thrust output by optimizing the thrust-producing blade area.

3.2 Acoustic performance

In terms of noise emission, both the 7x4 SF APS Propeller and the 6040 NACA2415 Classic Propeller presented a similar and consistent reading, achieving a sound level of 86.7 dB at the elevated rotational speed of 11 000 RPM.

Not notably, the 6040 NACA2415 TriLoop Toroidal Propeller displayed a negligible lower noise level of 86.6 dB, which could be attributed to the accuracy and resolution of the measuring equipment. However, it was evident that this propeller suffered from significant balance issues leading to additional noise generation through vibrations as can be seen in **Figure 3** around the 1300 µs PWM value. This imbalance adversely affected the propeller's acoustic performance despite its extremely marginal improvement in noise reduction at the maximum speed.

In contrast, the 6040 NACA2415 Toroidal Propeller emerged as the most acoustically efficient among the tested configurations. It achieved a noise level of 85.6 dB, surpassing the other propellers. Moreover, the 6040 NACA2415 Toroidal Propeller exhibited smoother and more stable operation, with reduced vibrations compared to the 6040 NACA2415 TriLoop Toroidal Propeller. Nevertheless, it was observed that the acoustic performance of the 6040 NACA2415 Toroidal Propeller did not match the near-perfect balance exhibited by the 7x4 SF APS Propeller or the 6040 NACA2415 Classic Propeller.

3.3 Efficiency

In addition to the examination of maximum thrust values, we assessed the power efficiency of each propeller type. This involved calculations in which the measured thrust (force) data was divided by the concurrently measured data of power consumption (product of load voltage and current) for each measurement.
The results revealed that despite variations in RPM ranges, all propellers displayed relatively proximate power efficiency values, deviating from one another by less than 4%. The minimal deviations in power efficiency suggest that each propeller design has been optimized to efficiently harness the available energy for specific thrust generation and thus achieve specific volumetric flow.
However, the 7x4 SF APS Propeller stood out with a notably better overall efficiency range (if compared to the ranges in which the toroidal propellers started to lose momentum (suffer)).

3.4 Other observations

During the experimental measurements, we observed a notable increase in the temperature of the motor when testing the toroidal propellers. The elevated temperature can be attributed to the higher mass of the toroidal propeller and extra vibrations due to balancing issues, which can be observed in **Figure 3**. The higher mass of the toroidal propellers requires an augmented amount of rotational energy to accelerate to the desired RPM, leading to more substantial mechanical loading on the motor. This increased mechanical loading poses potential challenges to the motor's durability and performance in extended operational scenarios.

Additionally, the experimental results revealed that toroidal propellers exhibit longer ramp-up and deceleration times in achieving and adjusting RPM levels. Through analysis of the audio spectre, we have observed that toroidal propellers exhibit longer ramp-up times when subjected to a newly generated thrust PWM

signal. This phenomenon is attributed to the higher inertia resulting from the increased mass of the toroidal propellers. Consequently, it takes comparatively more time for the motor to impart the required rotational energy to the toroidal propellers and bring them up to the desired RPM. Similarly, during deceleration, the higher inertia of the toroidal propellers leads to a slower decrease in RPM, requiring extended periods for RPM adjustments.

Such delays in achieving and adjusting RPM could be particularly critical in applications where precise and rapid RPM control is vital, such as in vehicles that utilise propellers for stabilisation, such as drones. The longer ramp-up and deceleration times, varying within the range of 5-20 milliseconds per ramp-up, could potentially affect the manoeuvrability, stability, and control of such vehicles. It may pose challenges in executing quick and accurate response commands, leading to potential stability issues and hampering the vehicle's ability to maintain desired positions or trajectories.

4 Conclusion

The experimental analysis revealed several differences between classic and toroidal propellers. Toroidal propellers demonstrated better maximum power per specific diameter. However, they also imposed greater mechanical stress on the motor due to their increased mass, leading to longer ramp-up and deceleration times for RPM adjustments. Classic propellers, on the other hand, showed consistent performance and stability in terms of thrust generation and mechanical stress. Further research and design optimization is essential to harness the advantages of toroidal propellers while addressing their challenges for enhanced propulsion systems.

The results underscore the significance of propeller design considerations, especially when exploring the potential of toroidal propellers in various industries and domains.

An interesting observation during the experimentation was the occurrence of vibrations and instability in the toroidal propellers. These observed anomalies led to a decrease in thrust output and noticeable acoustic differences at specific RPM, which were not detected in the classic propellers. Resonance phenomena can significantly impact the propeller's performance and efficiency by causing inefficient energy transfers and vibrations. The presence of resonance frequencies in toroidal propellers underscores the importance of dynamic analysis and consideration of vibrational behaviour during their design and optimization. Identifying and addressing potential resonance anomalies is critical to ensuring stable and efficient operation, especially in applications where precision and consistent performance are essential.

However, it is crucial to acknowledge the limitations of this preliminary study. One notable limitation was the absence of testing varied classic propellers with a higher blade count. Exploring classic propellers with different blade configurations could have provided valuable comparative data, potentially revealing insights that might have drawn closer comparisons to toroidal propellers.

5 Acknowledgement

I extend my heartfelt appreciation to all individuals who contributed their expertise, guidance, and encouragement throughout this journey. Moreover, I am grateful to the esteemed MIT Lincoln Laboratory for its inspiration and instrumental role in igniting the spark that initiated this research work. Their innovative contributions and cutting-edge ideas have been the driving force behind this endeavour.

6 References

[1] MATT FERRELL and JON OKUN, “Why is this Propeller Getting So Much Attention?,” *Undecided*, May 02, 2023. https://undecidedmf.com/why-is-this-propeller-getting-so-much-attention/ (accessed Jul. 28, 2023).

[2] D. Almazo, C. Rodríguez, and M. Toledo, “Selection and design of an axial flow fan,” *World Academy of Science, Engineering and Technology International Journal of Aerospace and Mechanical Engineering*, vol. 7, no. 5, pp. 923–926, 2013.

[3] N. Landell-Mills, “Propeller thrust explained by Newtonian physics,” *Pre-Print DOI*, vol. 10, 2021.

[4] MIT Lincoln Laboratory, “Toroidal Propeller,” *INNOVATION HIGHLIGHT*, 2022. https://www.ll.mit.edu/sites/default/files/other/doc/2023-02/TVO_Technology_Highlight_41_Toroidal_Propeller.pdf (accessed Jul. 28, 2023).

[5] I. O. N. Gabriel and I. SIMION, “PERFORMANCE OF 3D PRINTED CONVENTIONAL AND TOROIDAL PROPELLER FOR SMALL MULTIROTOR DRONES,” *Journal of Industrial Design and Engineering Graphics*, vol. 18, no. 1, pp. 27–32, 2023.

[6] “Airfoil Tools: NACA 2415 (n2415-il),” *Airfoil Tools*. http://airfoiltools.com/airfoil/details?airfoil=n2415-il. (accessed Jul. 28, 2023).

[7] 3DJAKE, “Technical Data Sheet,” Oct. 2020. Accessed: Jul. 28, 2023. [Online]. Available: https://c-3d.niceshops.com/upload/file/Technical_Data_Sheet[12].pdf